ELSEVIER

Journal of Power Sources 83 (1999) 193–203

JOURNAL OF POWER SOURCES

www.elsevier.com/locate/jpowsour

Impedance, power, energy, and pulse performance characteristics of small commercial Li-ion cells

G. Nagasubramanian *, R.G. Jungst, D.H. Doughty

Lithium Battery Research and Development Department 2521, Sandia National Laboratories, Albuquerque, NM 87185-0613, USA

Received 19 February 1999; accepted 27 April 1999

Abstract

Electrochemical properties of cylindrical (18 650, 17 500) and prismatic (48.3 × 25.4 × 7.6 mm) Li-ion cells from different manufacturers including A&T, Panasonic, Polystor, Sanyo, and Sony were studied. Impedance and pulse characteristics of these cells were evaluated for three open circuit voltages (OCVs): 4.1 V (fully charged), 3.6 V (partially discharged), and 3.1 V (nearly completely discharged) in the temperature regime +35°C to −40°C. The cell ohmic resistance was nearly constant from +35°C to −20°C, but increased by 2–3 times at −40°C. For example, the cylindrical Sony cells showed an average bulk resistance of ~80 mΩ between 35°C and −20°C and ~290 mΩ at −40°C for the three OCVs studied. The cell ohmic resistance remained nearly constant with OCV. The NyQuist plot (real vs. imaginary impedance) showed, at high frequencies (2.7–65 kHz), an inductive segment characteristic of a porous electrode and/or a jelly-roll cell design. The NyQuist plots also showed two ill-defined loops, a smaller loop at higher frequencies attributed to the anode electrolyte interface and a larger loop at lower frequencies due to the cathode electrolyte interface. A smaller charge transfer resistance (R_{ct}) at the anode is indicated and the performance of the cell may be improved by reducing the interfacial resistances, in general. Ragone plots, relating energy density and power density or specific power and specific energy, were also constructed to compare the performance characteristics of these cell types. In the current range studied (20–1000 mA), the energy/power performance of both A&T and Panasonic cells is better than the rest. For these two cells, the power (W/kg or W/l) didn't reach a plateau in the current range studied. These data should be considered, however, in the context that the A&T and Panasonic cells may be newer (later generation) than the other cells used in this study. However, at higher currents (> 2 A) and at lower temperatures, for the Panasonic cells, power reaches a plateau. This behavior is also true for the A&T cells. The cells were pulsed at different temperatures both as a function of OCV and current pulse amplitude. The cell voltage drop is almost linear with pulse current at ambient and slightly subambient temperatures. However, at lower temperatures, the voltage drop is nonlinear with pulse current, suggesting that the contribution of charge transfer resistance to the overall cell impedance under load is nontrivial. In addition, the cell voltage drop for a given current pulse increases with depth of discharge. For example, for a 500 mA pulse at 4.1 V, 3.6 V, and 3.1 V, the Panasonic cells showed an average voltage drop of 94 mV, 130 mV, and 200 mV, respectively, at room temperature. A similar observation was made for the other Li-ion cells.

Keywords: Li-ion; Ragone data; Impedance

1. Introduction

A highly reliable rechargeable battery of high power and energy is critically needed for a variety of new and exciting technologies. In principle, a high-voltage and high-specific energy battery is achievable by using a low-equivalent weight electropositive element in the battery. Because of its low equivalent weight (6.941) and high electrochemical standard potential (−3.038 V vs. normal hydrogen electrode), lithium metal is an attractive material for high-specific energy batteries. The low equivalent weight results in a specific capacity of 3.8 Ah/g, which is higher than other anode materials like lead (0.26 Ah/g) and the high electrochemical standard potential yields higher cell voltage (~4.1 V) compared to other batteries like Ni/MH (1.2 V). The commercialization of lithium primary batteries was achieved fairly quickly in the 1960s and 1970s. However, the development of lithium rechargeable batteries was much slower because of safety problems due to cell failure caused by lithium dendrite formation [1] and aggravated by the reactivity of high-area lithium powders formed by cycling. To overcome this problem, several possible alternatives to metallic lithium have been studied

* Corresponding author. Tel.: +1-505-844-1684; fax: +1-505-844-6972; E-mail: gnagasu@sandia.gov

0378-7753/99/$ - see front matter
PII: S0378-7753(99)00296-7

Table 1
Physical characteristics and capacities of Li-ion cell types

Manufacturer	Cell type and dimensions (mm)	Rated cell capacity (mAh)	Measured discharge capacity (mAh) at $C/20$	Weight (g)	Volume (l)	Number of cells tested
A&T	Cylindrical (17 500)	800	750	25.98	0.0106	3
Panasonic	Cylindrical (17 500)	780	751	24.13	0.0090	3
Polystor	Cylindrical (18 650)	1250	1133	43.76	0.0168	3
Sanyo	Cylindrical (18 650)	1300	1358	46.46	0.0202	2
Sanyo	Prismatic (48.3 × 25.4 × 7.6 mm)	550	508	20.03	0.0093	2
Sony	Cylindrical (18 650)	1100	1100	40.14	0.0171	5

[2,3], but with very little success in the past. However, a promising material based on carbon as an alternative to metallic lithium and lithium alloys has been proposed recently. This involves an innovative design (called rocking-chair or shuttlecock) in which lithium ions shuttle between the anode and the cathode. During discharge, lithium ions move from the anode into the cathode and during charge, lithium ions move from the cathode into the anode. There is no deposition of metallic lithium on the anode surface as in the case of lithium metal rechargeable batteries and therefore, Li-ion batteries are very safe. This idea was incorporated and developed by Sony to produce the so-called Li-ion cells for commercial applications [4,5]. The Sony cell is based on the rocking-chair concept and is composed of a lithiated carbon anode, a $Li_{1-x}CoO_2$ cathode and a nonaqueous electrolyte. Other manufacturers are producing cells with variations of the same basic chemistry. These batteries can store three times more energy per unit weight and volume than conventional systems (lead–acid and nickel/cadmium). Because of the high energy ($\sim$ 100 Wh/kg; $\sim$ 240 Wh/l), Li-ion batteries are finding widespread use in a variety of devices including computers, cellular phones, power tools, implantable medical devices, etc., and are being proposed for use in military, space, and electric vehicle applications, all of which have unique requirements. For example, computers and power tools may need short bursts of high power, whereas implantable devices may require low current (power) for a long period of time.

When evaluating battery suitability for such unique applications, one needs to know a variety of battery characteristics, including the energy/power relationship (Ragone plot), cell impedance as a function of temperature, pulse discharge capability as a function of both temperature and load, and charge/discharge characteristics. Although there are a few published data on the

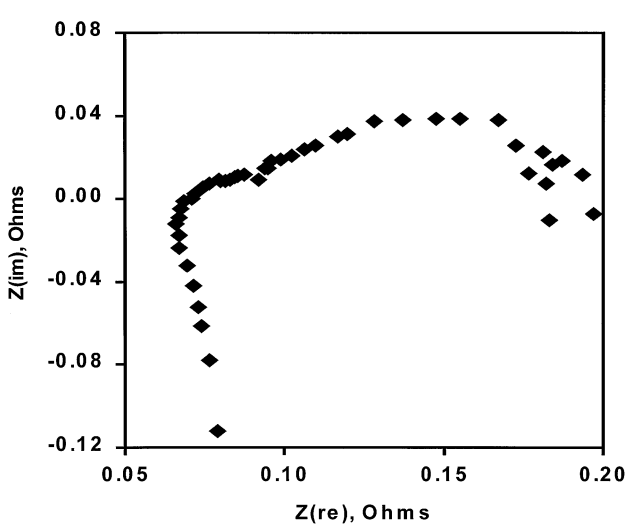

Fig. 1. NyQuist plot for a fully charged Sony cell (OCV = 4.1 V). The impedance was measured at room temperature.

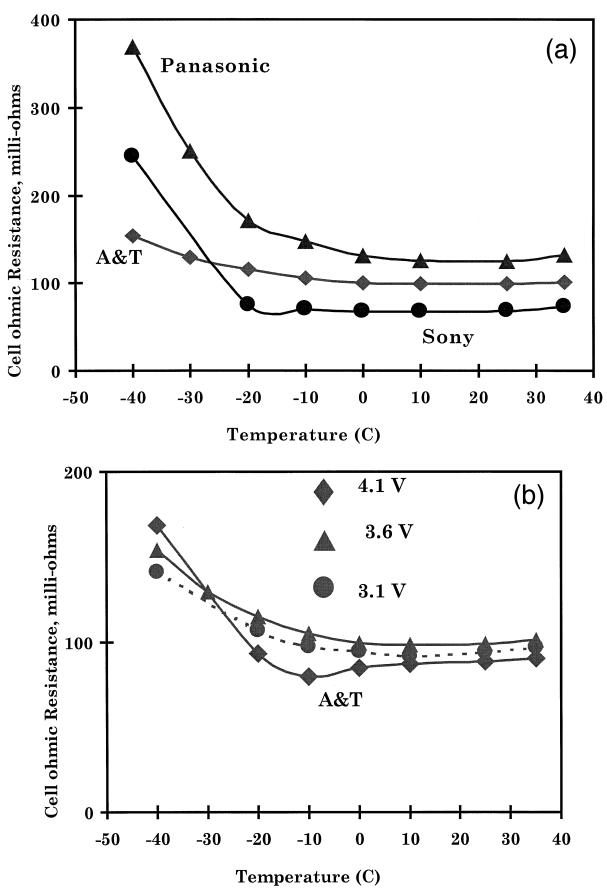

Fig. 2. (a) Average ohmic resistance of the A&T, Panasonic, and Sony cells at 4.1 V OCV as a function of temperature. (b) Average ohmic resistance of the A&T cells as a function of temperature and OCV.

Table 2
Total impedance (Ohms) as a function of temperature and OCV

Temperature (C)	A&T	Panasonic	Polystor	Sanyo cylindrical	Sanyo prismatic	Sony
4.1 V						
−40	14.30 *(0.15)*	8.84 *(0.37)*	2.33	4.92	3.54	7.87
−30	6.43 *(0.13)*	7.24 *(0.25)*	0.84	1.53		
−20	2.58 *(0.12)*	3.87 *(0.17)*	0.41	0.52	0.91	1.58
−10	0.98 *(0.11)*	1.65 *(0.15)*	0.26	0.22	0.56	1.37
0	0.45 *(0.10)*	0.76 *(0.13)*	0.17	0.17	0.46	0.78
+10	0.26 *(0.10)*	0.39 *(0.13)*	0.16	0.14	0.40	0.38
+25	0.16 *(0.10)*	0.23 *(0.13)*	0.22	0.14	0.42	0.18
+35	0.13 *(0.10)*	0.20 *(0.13)*	0.19	0.14	0.39	0.14
3.6 V						
−40	14.44	9.60	2.28	2.80	3.82	9.34
−20	3.02	4.02	0.38	0.49	0.94	1.24
−10	1.45	1.85	0.22	0.33	0.60	1.25
0	0.59	0.88	0.16	0.27	0.45	0.91
+10	0.29	0.53	0.18	0.24	0.42	0.46
+25	0.17	0.30	0.22	0.25	0.41	0.20
+35	0.14	0.24	0.21	0.25	0.42	0.15
3.1 V						
−40	23.29	9.08	5.30	4.50	27.82	12.75
−20	5.13	3.88	0.60	0.71	1.12	1.76
−10	2.42	1.45	0.39	0.44	0.73	1.22
0	1.13	0.72	0.30	0.36	0.49	1.13
+10	0.51	0.52	0.23	0.33	0.45	0.61
+25	0.28	0.42	0.24	0.34	0.40	0.28
+35	0.19	0.36	0.21	0.30	0.45	0.18

charge/discharge characteristics of Li-ion cells [6–8], a comprehensive investigation of the relevant electrochemical characteristics for use by battery designers is not, to our knowledge, currently available in the literature. This paper describes measurements of some of the fundamental electrochemical characteristics such as impedance, power, energy, etc., of commercial Li-ion cells of different sizes (18 650, 17 500, cylindrical and prismatic) from different manufacturers and compares their properties.

2. Experimental

Li-ion cells of three different sizes (18 650, 17 500, cylindrical and $48.3 \times 25.4 \times 7.6$ mm prismatic) were

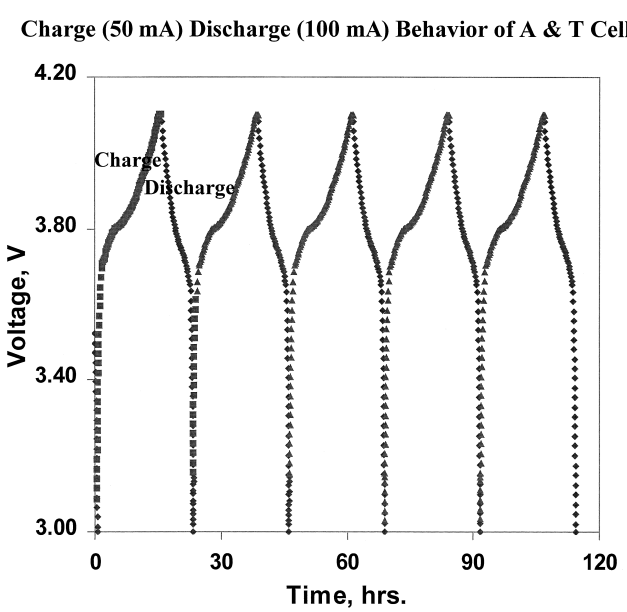

Fig. 3. Charge/discharge characteristics of an A&T cell at room temperature. Charge current = 50 mA, discharge current = 100 mA.

Table 3
Discharge capacity (mAh) as a function of temperature and discharge current

Cell	Temperature (°C)	100 mA	200 mA	500 mA	750 mA
A&T	+25	730	731	727	721
	+10	718	708	681	673
	−10	669	641	–	–
Panasonic	+25	751	750	742	733
	+10	746	744	705	679
	−10	672	650	–	–

evaluated. Before welding tabs to the cells for electrical connections, both their weights and physical dimensions were measured. These weights and computed cell volumes are given in Table 1 along with the cell type, capacity, manufacturer, and the number of cells tested. Initially, the cells were charged and discharged at room temperature (for at least five cycles) at a very low rate ($\sim C/20$) as 'break-in' cycles. The discharge capacity given in Table 1 represents the average of five cycles per cell and is also averaged over the number of cells tested for that type. The nominal (rated) cell capacity is slightly higher than the measured discharge capacity except for the Sony and Sanyo cylindrical cells. While the exact reason for this difference is not known, it is very likely that the A&T, Panasonic, Polystor, and Sanyo Prismatic ratings are not for cells that are fully conditioned for the irreversible losses of the anode. The cells were charged and discharged at different currents ranging from 20 mA to 1.0 A using an Arbin battery cycler (Model BT2042, College Station, TX). The charge/discharge measurements were also carried out at different temperatures and cell temperatures during tests were controlled with a Tenney Jr. temperature chamber (benchtop model, Union, NJ). For cell impedance measurement, a Princeton Applied Research (PAR) 273A potentiostat in conjunction with a 1255 Solatron Oscillator (Model 378) was used. The impedance of the Li-ion cells was measured from 65 kHz to 0.1 Hz as a function of temperature for three different open circuit voltages (OCVs). For current pulse measurement, a 273A PAR potentiostat/galvanostat was used and the voltage response was captured with a Tektronix Oscilloscope (Model # THS 720). The pulse data stored in the oscilloscope were transferred to a computer using a 'Wavestar' program (version 1-0-3) for data processing and plotting. We waited around 30 min between pulses.

3. Results and discussion

3.1. Impedance characteristics

A typical NyQuist plot (real vs. imaginary impedance) for a fully charged (OCV = 4.1 V) Sony cell at 25°C is shown in Fig. 1. It has an inductive tail in the frequency regime 2.7–65 kHz and then a small loop followed by a larger loop. The inductive tail has been observed by others for Li-MoS_2 cells [9] and in that case, has been attributed to the jelly-roll and/or porous electrode designs. The inductive tail in the case of the Sony cell could also be due

Table 4
Ragone data for A&T cell at room temperature[a]

Cell parameters	Charge 50 mA, discharge 100 mA	Charge 100 mA, discharge 200 mA	Charge 200 mA, discharge 500 mA	Charge 500 mA, discharge 750 mA	Charge 500 mA, discharge 1000 mA
Capacity (mAh)	730	731	727	721	717
Specific Energy (Wh/kg)	106.48	106	103.1	100.9	99.1
Specific Power (W/kg)	14.2	27.9	69.4	103.7	137.6
Energy Density (Wh/l)	261.5	260.3	253.3	247.8	243.3
Power Density (W/l)	34.8	68.6	170.3	254.7	338

[a]Weights and volumes of cells are given in Table 1.

Table 5
Ragone data for Panasonic cell at room temperature[a]

Cell parameters	Charge 50 mA, discharge 100 mA	Charge 100 mA, discharge 200 mA	Charge 100 mA, discharge 250 mA	Charge 200 mA, discharge 500 mA	Charge 500 mA, discharge 750 mA	Charge 500 mA, discharge 1000 mA
Capacity (mAh)	751	751	750	742	733	720
Specific Energy (Wh/kg)	117.6	116.5	116	112.7	109.4	105.4
Specific Power (W/kg)	15	29.5	36.6	72.6	108.2	143.2
Energy Density (Wh/l)	315.3	312.3	311.1	302.1	293.2	282.6
Power Density (W/l)	40.3	79	98.2	194.6	290	383.8

[a]Weights and volumes of cells are given in Table 1.

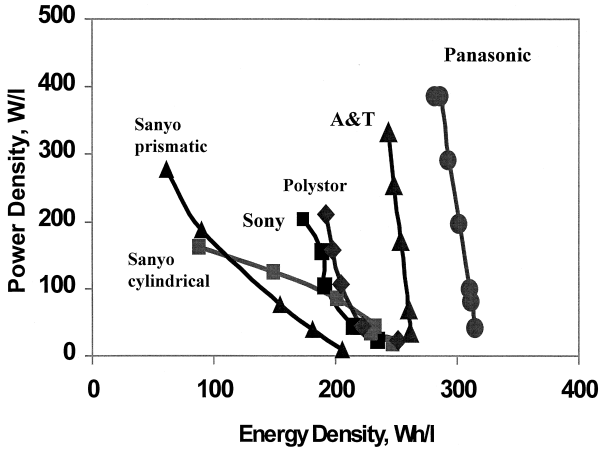

Fig. 4. Ragone plot of energy density vs. power density at room temperature for the Li-ion cells.

to a similar design feature. Based on our three electrode impedance data, it appears that the cathode/electrolyte interface impedance dominates the overall cell impedance. The first impedance loop in Fig. 1 is assigned to the anode electrolyte interface and the second loop to the cathode electrolyte interface based on published data in the lithium rechargeable area [10] and also on carbon single electrode studies [11]. The ohmic cell resistance (high frequency *x*-axis intercept), which includes electrolyte resistance and other resistances such as electrode bulk resistance, separator resistance, etc., in series with it, is small ($\sim 0.08\ \Omega$). However, the overall cell impedance including ohmic resistance, anode electrolyte R_{ct} and cathode electrolyte R_{ct} is significant ($\sim 0.18\ \Omega$). It is clear from Fig. 1 that the contribution to the cell impedance from the cathode electrolyte interface is nontrivial. The implication of this observation is that there is room to improve the power output of the cell further by optimizing the cathode electrolyte interface to reduce the interfacial resistance. Similar impedance behavior was observed for the other cells. In Fig. 2a, the average cell ohmic resistance as a function of temperature at OCV = 4.1 V for some of the cells included in this study is given. The cell ohmic resistance is nearly constant from 35°C to −20°C, but by −40°C, the resistance has increased by 2–3 times. In Fig. 2b, the cell ohmic resistance for the A&T cell at the three OCVs is given. The cell ohmic resistance was also nearly constant with OCV except for Sanyo cylindrical cells (not shown in the figure), where the resistance increased marginally going from fully charged to almost fully discharged. This observation implies that the bulk conductivity of the components is not seriously affected by the state of charge. Further, the bulk electrolyte resistance is low enough that it may not be the dominant factor controlling the power characteristics of the cell even at subambient temperatures. Although the cell ohmic resistance remains constant from 35°C to −20°C in all cases, the total cell impedance increases as the cell temperature goes down (with corresponding increases in the 1st and 2nd loops in the NyQuist plots). The main contribution to the total cell impedance therefore comes from the interfacial resistances. In Table 2, the total cell impedance for the Li-ion cells both as a function of temperature and OCV is shown. It can be seen that the total cell impedance is very high, especially at lower temperatures, compared to the cell ohmic resistance (vide Fig. 2). For comparison purposes, the cell ohmic resistances for the A&T and Panasonic cells are given for 4.1 V in parenthesis along with the total cell resistances in Table 2. The difference is due to the contribution from the

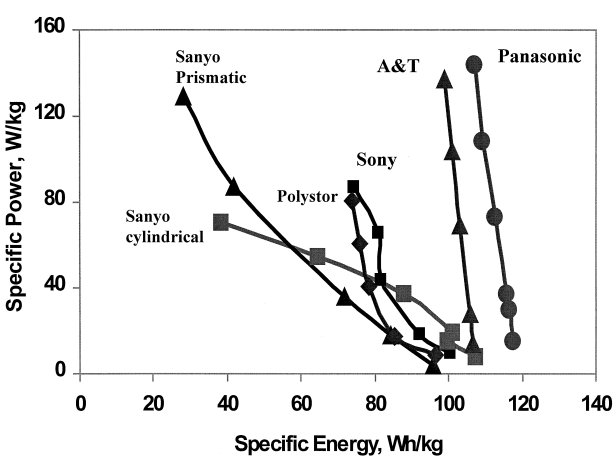

Fig. 5. Ragone plot of specific energy vs. specific power at room temperature for the Li-ion cells.

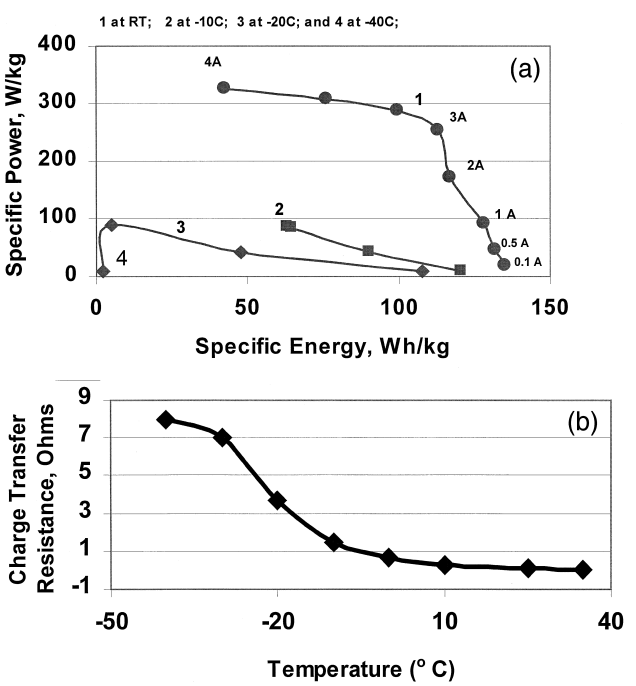

Fig. 6. (a) Ragone plot of specific energy vs. specific power at different temperatures for the Panasonic Li-ion cells. Discharge currents are given in the figure. (b) R_{ct} vs. Temperature (°C) for Panasonic Li-ion cell at different temperatures.

interfacial charge transfer and diffusional resistances. The importance of the interfacial resistance to the overall cell performance is described further below. We will discuss this taking the A&T and Panasonic cells as examples.

3.2. Discharge capacity

In Fig. 3, typical charge/discharge curves for an A&T cell at room temperature for a 50 mA charge and 100 mA discharge are given. The coulombic efficiency (charge in/charge out) computed from the charge/discharge curves is equal to one, which indicates that the only electrochemical processes that are occurring in the cell are the intercalation and deintercalation reactions. Further, it indicates that there is complete freedom from parasitic side reactions that could degrade the cell performance. The charge/discharge measurements were made at three different temperatures for all the cells. In Table 3, the discharge capacity of A&T and Panasonic cells both as a function of temperature and discharge rate is shown. As expected, the delivered capacity is lower at lower temperatures and at higher rates. This behavior is also typical of the other cells. The discharge energy and power computed from the discharge curves at different rates are normalized to weight and volume (from Table 1) and assembled in Tables 4 and 5 for the A&T and Panasonic cells at room temperature. Again the results are averaged over five cycles per cell and the number of cells tested for that type. The specific power as well as the power density are high and didn't reach a plateau even at the highest discharge rates tested. The data also indicate that these cells can be charged and discharged at very high currents (>1 A) [12]. Discharge energy and power data were also obtained for the Li-ion cells of other manufacturers. All of these data are given in the form of Ragone plots in Figs. 4 and 5. The Ragone plots, first reported by Ragone [13], relate power density (or specific power) to obtainable energy density (or specific energy), and are a useful tool for comparative performance evaluation of different battery systems.

In Fig. 4, power density vs. energy density for all of the cells studied is plotted. As mentioned above, the electrical performances of the A&T and Panasonic cells are impressive. However, the energy and power characteristics of the tested cells from other manufacturers (Polystor, Sanyo, and

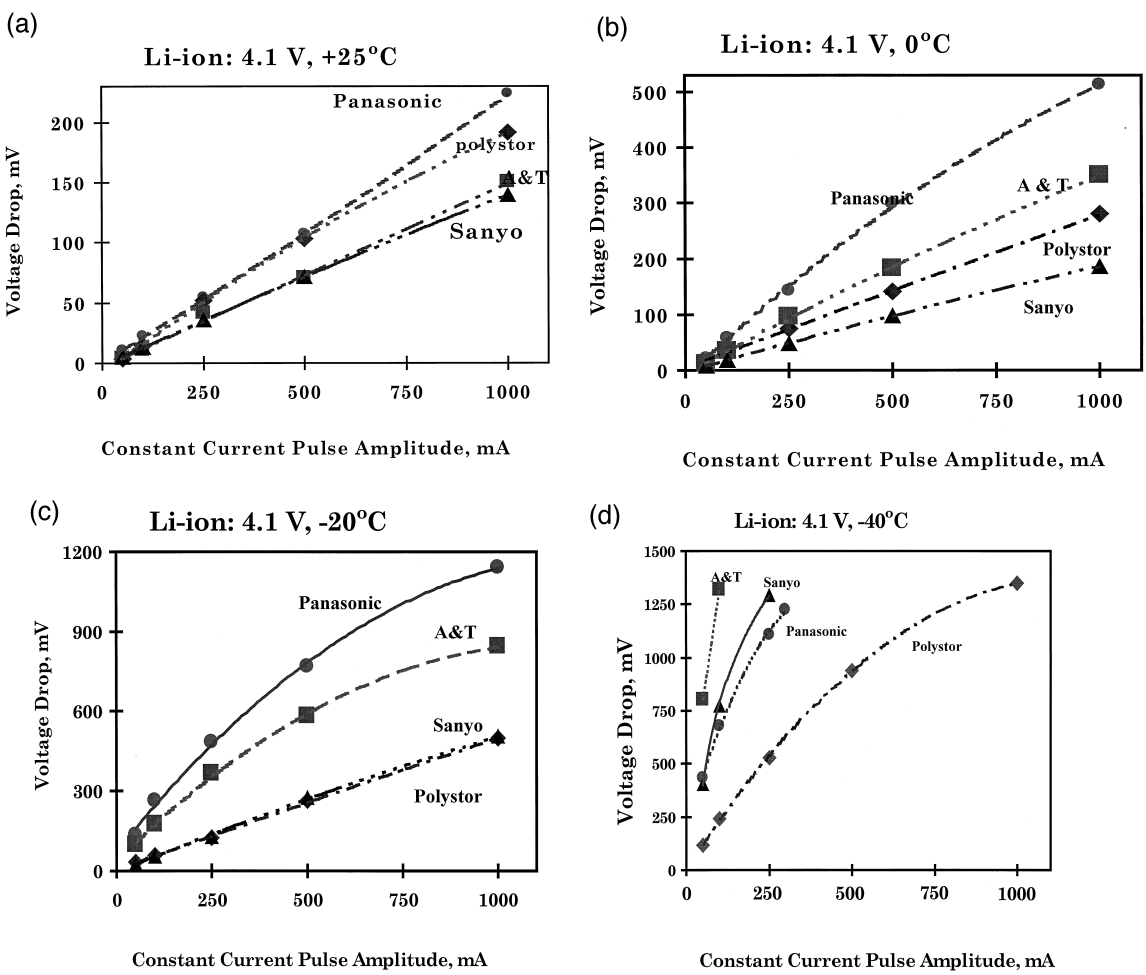

Fig. 7. Cell voltage drop for fully charged A&T, Panasonic, Polystor, and Sanyo (cylindrical) cells at room temperature as a function of current pulse amplitude. Pulse duration = 1 s. (a) 25°C, (b) 0°C, (c) −20°C, and (d) −40°C.

Table 6
Voltage drop for different pulse currents as a function of temperature and OCV

Current (mA)	A&T (mV)	Panasonic (mV)	Polystor (mV)	Sanyo (mV)	Sanyo prismatic (mV)	Sony (mV)
4.1 V						
35°C						
50	1	7	2	2		
100	10	10	10	12		
250	29	37	36	27		
500	57	79	85	70		
1000	120	174	170	120		
25°C						
50	4	10	4	5	5	1
100	10	16	15	13	30	6
250	41	46	52	36	69	29
500	70	94	103	72	137	37
1000	150	212	192	140	297	95
10°C						
50	14	21	12	10	11	1
100	15	30	30	13	27	8
250	54	82	68	36	73	25
500	110	164	125	77	173	63
1000	237	327	239	145		
0°C						
50	12	26	12	9	13	5
100	35	54	40	18	27	14
250	96	146	74	49	78	54
500	183	294	142	98		
1000	350	517	280	187		
−10°C						
50	44	62	22	10	13	5
100	82	124	40	27	27	15
250	192	295	89	59	91	45
500	345	485	170	117		
1000	577	784	348	248		
−20°C						
50	99	143	32	27	14	4
100	175	258	59	57	33	20
250	366	492	124	129	123	89
500	580	770	262	275		
1000	843	1149	498	505		
−30°C						
50	214	272	50	105		
100	350	437	93	238		
250	621	764	217	684		
500	877	1120	437	1322		
1000	1128		795			
−40°C						
50	802	433	115	402		353
100	1318	674	242	773		610
250		1129	529	1291		1210
500		1226 (300 mA)[a]	938			
1000			1348			
3.6 V						
35°C						
50	5	10	10	10	15	10
100	5	10	10	15	30	10
250	18	40	30	55	90	30
500	53	90	80	115	195	70
1000	138	195	160	239	380	130

Table 6 (continued)

Current (mA)	A&T (mV)	Panasonic (mV)	Polystor (mV)	Sanyo (mV)	Sanyo prismatic (mV)	Sony (mV)
3.6 V						
25°C						
50	8	10	10	10	20	10
100	10	25	10	20	37	15
250	32	60	45	70	105	50
500	73	130	100	125	210	100
1000	153	225	175	240	400	180
10°C						
50	10	20	10	10	20	19
100	25	45	20	20	40	40
250	60	110	59	70	115	90
500	136	207	112	120	230	184
1000	253	410	230	250	447	320
0°C						
50	25	30	10	10	25	39
100	45	70	20	20	49	60
250	115	180	70	70	129	157
500	235	350	142	130	252	280
1000	406	585	270	275	500	430
−10°C						
50	55	74	10	20	32	57
100	105	140	29	25	59	102
250	235	332	80	80	159	242
500	406	530	159	165	303	380
1000	624	689 (750)[a]	320	320		600
−20°C						
50	125	160	20	29	50	80
100	220	280	42	49	85	160
250	430	550	127	129	225	358
500	655	709 (400)[a]	242	262	430	584
−40°C						
50	500	443	125	170	249	390
100	768	700	220	320	347	665
250			488			
3.1 V						
35°C						
50	10	15	10	17	23.3	10
100	10	30	10	23	35	10
250	42	73	38.3	70	100	40
500	80	138	80	160	203	80
1000	165	243	175	320	420	175
25°C						
50	15	27	10	25	20	13
100	25	40	20	28	43.3	22
250	70	123	53.3	83	105	62
500	118	200	101.7	163	215	125
1000	215	320	210	340	425	230
10°C						
50	15	27	10	10	25	28
100	40	55	20	25	38.3	47
250	115	150	73.3	80	125	132
500	220	267	147	162	252	222
1000	372	453	280	342	472	300 (800)[a]
0°C						
50	50	40	22	15	30	37
100	80	80	40	30	55	70

Table 6 (continued)

Current (mA)	A&T (mV)	Panasonic (mV)	Polystor (mV)	Sanyo (mV)	Sanyo prismatic (mV)	Sony (mV)
3.1 V						
250	190	230	90	92	132	190
500	347	407	180	190	277	348
1000	543	640	340	375	540	
−10°C						
50	92	90	28	30	40	60
100	168	165	42	40	62	128
250	345	367	122	110	175	297
500	523.3	600	240	218	343	
1000				438	662	
−20°C						
50	178	165	30	83	50	98
100	308	287	70	185	97	198
250	550	560	193	478	250	
500			342	500	452	
−40°C						
50	843	465	720	570		475
100		708				

[a] Denotes that the voltage drop was measured for the current given in the bracket and not at the current value given at the leftmost column.

Sony) are inferior to those of the A&T and Panasonic cells. For the Sanyo cylindrical cells, the power density reaches a plateau below 200 W/l. Between the two Sanyo Li-ion cell types, the prismatic cell exhibits higher power density than the cylindrical cell. The electrical performance of Sony cells is comparable to that of the Polystor cells. Specific energy vs. specific power data shown in Fig. 5 indicates similar trends to those described above. In analyzing this data, one has to keep in mind that these cells from different manufacturers may not represent the same generation of cells. It is entirely possible that the A&T and Panasonic cells are from a later design than the rest. In Fig. 6a, Ragone data for the Panasonic cell at higher currents (~4 A) and at lower temperatures are given. At room temperature the delivered power reaches a maximum at higher currents, and at lower temperatures only lower currents discharges can be obtained. At −40°C, the delivered energy is nearly zero. This behavior reflects the increase in R_{ct} at lower temperatures. A plot of R_{ct} vs. temperature is given in Fig. 6b.

3.3. Operating characteristics under pulse loads

New applications such as digital wireless communications need pulse power so that more data can be packed into the available communication spectrum [14]. This demands very high current pulses for short durations from the battery pack. For example, Motorola cellular phones and NTT portable phones require current pulses on the order of 1000 mA for 0.6–7 ms. Keeping this and other applications in mind, we have evaluated the pulse performance characteristics of these cells for 1 s current pulses ranging from 50–1000 mA as a function of temperature and OCV. This technique has the advantage of measuring voltage for the complete cell under dynamic conditions. Fig. 7 shows the voltage drops at 4.1 V OCV for A&T, Panasonic, Polystor, and Sanyo cylindrical cells at several temperatures. The voltage drops as a function of temperature, OCV, and current are summarized in Table 6 for all of the cells investigated. Salient features emerging from the data are summarized below.

(1) The voltage drop at 25°C (Fig. 7a) for the four cells increases linearly with increasing current, which implies that the contribution from the ohmic resistance to the voltage drop is significant.

(2) At lower temperatures, especially for the A&T and Panasonic cells, the voltage drop is nonlinear, which suggests that the contribution from the interfacial/diffusional resistance is nontrivial. However, for the Sanyo and Polystor cells, the voltage drop is linear at 0°C and at −20°C which suggests that the contribution of the interfacial/diffusional resistance is not significant.

(3) At −40°C, all the cells show a nonlinear voltage drop.

(4) The voltage drop for a given current increases as the temperature goes down. For example, for a 100 mA pulse, the Panasonic cell showed a 16 mV drop at 25°C, a 258 mV drop at −20°C, and a 674 mV drop at −40°C. This is typical of the other cells.

(5) The voltage drop for the A&T cell is less than for the Panasonic cells for the higher temperatures studied, but at −40°C, the A&T cell voltage drop is higher than the Panasonic cell.

(6) A&T, Panasonic, and Sanyo cells cannot be pulsed at very high currents at −40°C.

(7) The voltage drop, for a current and temperature in general, increases slightly with depth of discharge (more depth of discharge means lower OCV). For example, at −20°C and 100 mA pulse, the Panasonic cells showed a voltage drop of 258 mV at 4.1 V OCV (fully charged); 280 mV at 3.6 V OCV (partially discharged); and 287 mV at 3.1 V OCV (nearly completely discharged).

(8) The cell resistance computed from the voltage drop is comparable to the total cell resistance obtained from the impedance measurement, especially near ambient temperature.

Observations #5 and #6 above cannot be explained if we just consider the cell's ohmic resistance (vide Fig. 2). A&T cells show a lower cell ohmic resistance at −40°C than the Panasonic cells at the same temperature. However, A&T cells show a higher voltage drop than the Panasonic cells at −40°C. One would not expect this trend since the ohmic resistance of the A&T cells is lower than the Panasonic cells at all temperatures. Further, the two cells should be able to be pulsed at higher currents since the ohmic resistance is only a few 100 mΩ. This clearly underscores the importance of the non-ohmic resistances such as interfacial charge transfer resistance and diffusional impedance in controlling the electrical and electrochemical properties of these cells. For example, the A&T cells show less than 200 mΩ ohmic resistance at −40°C. However, the total cell impedance for the same temperature is 14.3 Ω (vide Table 2). In this example, the interfacial resistance of ~14 Ω far exceeds the cell ohmic resistance, which is mainly due to the bulk electrolyte resistance. The impedance spectra at −40°C for the A&T and Panasonic cells are shown in Fig. 8. In Fig. 8a, the NyQuist plot of the impedance (real vs. imaginary) is shown; the Bode plot (real vs. frequency) of the same data is shown in Fig. 8b. The NyQuist plot shows two humps (indicated by arrows in the figure) as part of the 1st and 2nd semicircles corresponding to the anode and cathode, respectively, and also a straight line corresponding to diffusional impedance (Warburg impedance). These two humps can also be seen clearly in Fig. 1 for the Sony cell at room temperature. The first of the two loops is smaller than the 2nd, which implies that the charge transfer resistance at the cathode/electrolyte interface is higher than that at the anode/electrolyte interface. The DC resistance was computed by extrapolating the Bode plot data (Fig. 8b) to frequency = 0 and these values are reported in Table 2. The high total cell resistance explains why the voltage drop for the A&T cells is very large at −40°C. Again this emphasizes the importance of the non-ohmic resistances. At −40°C, the average total cell impedance for the Panasonic cells is only 8.84 Ω. The lower resistance of the Panasonic cell compared to the A&T cell at −40°C explains observation #5.

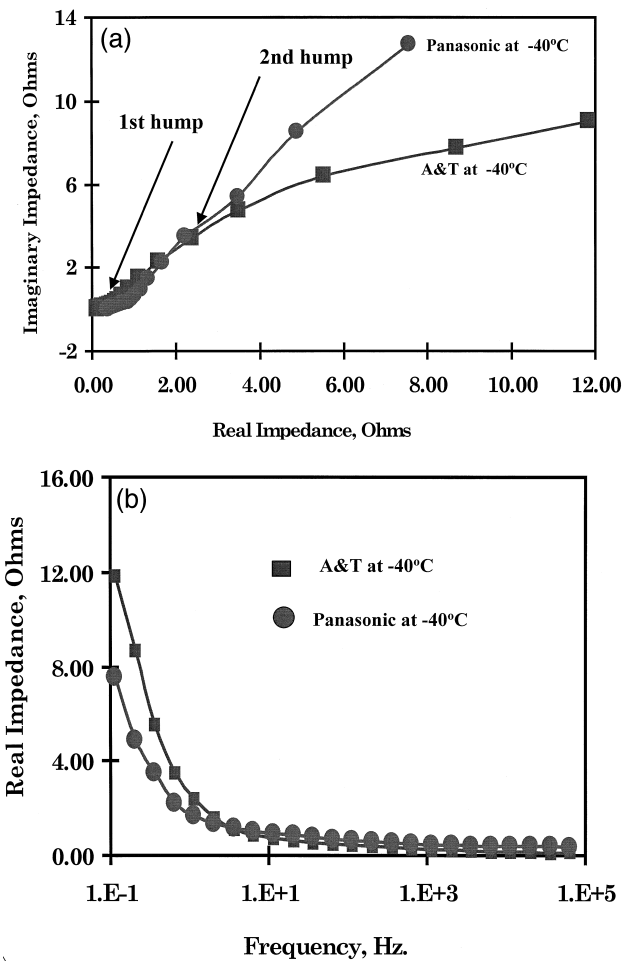

Fig. 8. Impedance plot for fully charged A&T and Panasonic cells at −40°C. (a) NyQuist plot (imaginary vs. real), and (b) Bode plot (real vs. frequency).

4. Conclusions

A number of Li-ion cells from different manufacturers were evaluated for their electrical and electrochemical characteristics as a function of temperature and OCV. Ohmic resistance remained nearly constant from 35°C to −20°C in all cases and then increased by 2–3 times at −40°C. The electrolyte resistance of the cells was only a few 100 mΩ, which is similar to that of Ni/Cd and Ni/MH cells of comparable size. Ohmic resistance was also nearly independent of state-of-charge (OCV). In the temperature range 35°C to −20°C, where the ohmic resistance remains almost constant, the voltage drop for a given current pulse increased with decreasing temperature. Although the ohmic resistance alone cannot explain this trend, the total cell impedance (including ohmic resistance, interfacial charge transfer resistances, and Warburg impedance) did increase with a decrease in temperature. The voltage drop for a given current and temperature roughly corresponds to the total cell impedance. Further, our impedance data indicate that the contribution from the

interfacial charge transfer resistance and diffusional impedance to the total cell impedance is quite significant at lower temperatures and the interfacial resistance of the cathode is higher than that of the anode. One has to keep this high R_{ct} of the cathode electrolyte interface in mind when optimizing the cell design for both high energy and power. Generally, the cell resistance computed from the voltage drop is comparable to the total cell resistance obtained from the AC impedance measurement, especially near ambient temperature. However, at lower temperatures, the voltage drop measurement yields a lower resistance, which might be due to an increase of the internal temperature of the cell caused by pulsing. We have also evaluated the charge/discharge characteristics of the cells at different temperatures and at different charge/discharge currents. The Ragone data obtained from measuring the discharge capacity at different discharge currents indicates that the Li-ion cells possess a favorable combination of energy and power at and near ambient conditions. The energy and power densities at room temperature could be as high as 320 Wh/l and 380 W/l, respectively. However, delivered energy and power (Ragone data) for the Li-ion cells at lower temperatures degrade very fast with very little delivered energy and power at -40°C.

Acknowledgements

Sandia National Laboratories is a multiprogram laboratory operated by Sandia Corporation, a Lockheed Martin Company, for the United States Department of Energy under contract DE-AC04-94AL85000. The authors also express their appreciation to suppliers who furnished evaluation hardware for this study. We are grateful to D.R. Bradley and H.L. Case for performing the electrochemical measurements.

References

[1] K.M. Abraham, Electrochim. Acta 38 (1993) 1233, and references therein.
[2] D. Fautux, R. Koksbang, J. Appl. Electrochem. 23 (1993) 1, and references therein.
[3] D.W. Murphy, P.A. Christian, Science 205 (1979) 651.
[4] O. Kazunori, M. Yokokawa, 10th Int. Seminar on Primary and Secondary Battery Technology Applications, 1–4 March, 1993, Deerfield Beach, FL, USA.
[5] Batteries International, Issue 31, April 1997, p. 12.
[6] Several papers on Li-ion Cells in Solid State Ionics, 69, 1994.
[7] B.A. Johnson, R.E. White, J. Power Sources 70 (1998) 48.
[8] G. Nagasubramanian, R.J. Jungst, J. Power Sources 72 (1998) 189.
[9] F.C. Laman, M.W. Matsen, J.A.R. Stiles, J. Electrochem. Soc. 133 (1986) 2441.
[10] J. Barker, R. Pynenburg, R. Koksbang, M.Y. Saidi, Electrochim. Acta 41 (1996) 2481.
[11] M.W. Wagner, Electrochim. Acta 42 (1997) 1623.
[12] E. Peter Roth, G. Nagasubramanian, 38th Power Sources Conference, 8–11 June, 1998, p. 512.
[13] D. Ragone, Proc. Soc. Automotive Engineers Conference, Detroit, MI, May, 1968.
[14] A. Anani, F. Eschbach, J. Howard, F. Malaspina, V. Meadows, Electrochim. Acta 40 (1995) 2211.